A Passive Fluid Valve Element for a High-density Chemical Synthesis Machine

Richard M. Moroney, Robert Amantea, and Sterling E. McBride

Sarnoff Corporation CN-5300 Princeton, NJ 08543
rmoroney@sarnoff.com, ramantea@sarnoff.com, smcbride@sarnoff.com

ABSTRACT

We have developed a passive valve element for use in a high-density chemical synthesis machine. The element stops fluid flow by the surface tension forces occurring at small channel openings. The openings are circular holes about 100 µm in diameter, referred to as capillary breaks. They have been built and tested in both glass and silicon; the holding pressure of the capillary break is on the order of 1500 Pa, or 5.9" of water column. Before yielding, the capillary break acts as an equivalent capacitance in the fluidic circuit. Details of the capacitance model are presented, along with supporting experimental work and computational fluid dynamics (CFD) simulations. This modeling lays the foundation for understanding the valve's operation in large arrays.

Keywords: arrays, microfluidics, surface tension, systems, valves.

INTRODUCTION

There has been general interest in microfluidics for some time now [1], including the idea that the larger relative magnitude of capillary forces might be used advantageously [2]. Much of the effort in microfluidics has been on genomics applications [3–5]; this work is motivated by a chemical synthesis application.

Drug discovery is an important pharmaceutical problem with potentially large payoffs. Combinatorial chemistry [6] is a relatively new approach to discovering novel drug compounds by synthesizing and screening a large number of different compounds at one time. Microfluidic systems offer the promise of reduced reagent needs, minimized waste products, and quicker, more efficiently generated compound libraries. We are working to create a 10,000 cell combinatorial chemistry synthesis machine. To achieve this high level of integration, we have developed a valve with no moving parts that can be fabricated in dense arrays. The valve has a passive element to stop flow (the "capillary break") and an active element to initiate flow (typically an EHD pump, described elsewhere [7]).

This paper will describe numerical simulations, experimental results, and analytical models used to design and understand the capillary break element.

THEORY

A cross-section of a possible design is shown in Figure 1a. The operating principle is that fluid flow stops at the channel opening due to surface tension forces. An initial concern was the range of contact angle allowed for proper operation. Simulations of the geometry in Figure 1a (a slot opening) were made with a detailed 2D model using the CFD code *FLUENT* [8] to gain insight into and understanding of the capillary flow. These showed that the vertical wall at the left of the opening prevents wetting fluids from stopping, as seen in Figure 1b. The design

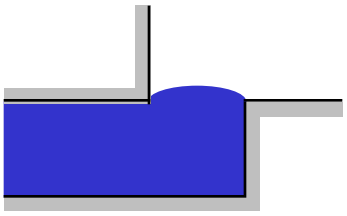

(a)

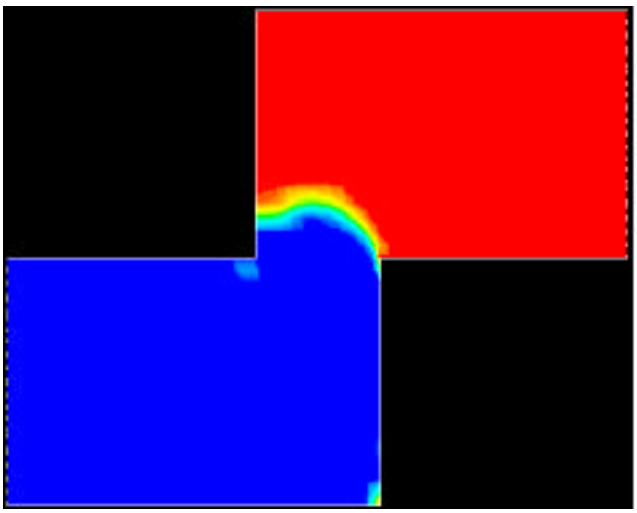

(b)

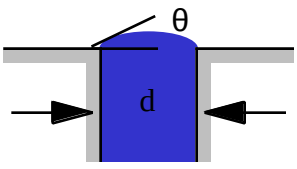

(c)

Figure 1: Cross section of a capillary break feature: (a) original concept, (b) simulation result, (c) working concept, with geometry details.

was modified to look like Figure 1c (a circular opening). This improved design has been validated in several different structures using typical organic synthesis solvents and reagents. Further CFD modeling showed that the flat shelf around the capillary opening needs to be on the order of the hole diameter in order to establish a stable meniscus.

There is a pressure drop across the meniscus due to its curvature given by the Laplace equation. For the spherical shape of Figure 1c, the pressure is

$$P = \frac{4\gamma \sin\theta}{d}, \qquad (1)$$

where γ is the surface tension, θ the contact angle, and d the diameter of the opening. This pressure is typically quite small; for γ = 0.037 N/m, d = 100 µm and θ = 90°, the pressure is 1500 Pa or 5.9" of water column.

EXPERIMENT

Experimental characterization has been done using individual channels with an inlet hole at one end and a single capillary break at the other. The setup is sketched in Figure 2. An off-chip reservoir is pneumatically pressurized with a resolution of 0.1" of water (25 Pa) to deliver fluids. The chip is mounted in a jig that connects to the fluid input and also has a gas input to dry off the capillary break between tests. The meniscus is observed either with a microscope or a laser displacement sensor.

Figure 3 shows results of yield pressure measurements using dimethylformamide (DMF) and capillary breaks made in glass that range from 120–140 µm in diameter.

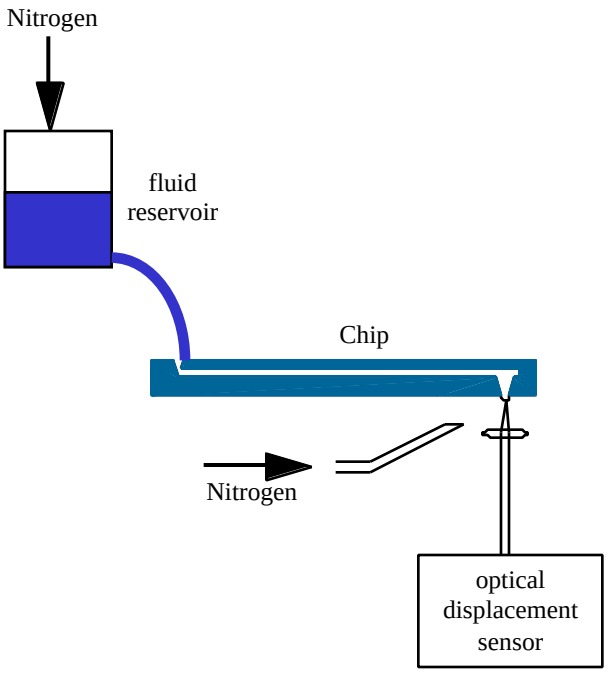

Figure 2: Experimental setup

Vertical error bars represent the variation from several measurements, and horizontal error bars represent the ellipticity of the holes; the curve is the expected pressure drop from Equation 1 using a contact angle of 43°.

A typical glass capillary break feature is shown in Figure 4a. The uneven edge of the hole is due to breakout from the fabrication process, which can be minimized but not eliminated. This contributes to the feature to feature variation in size and yield pressure seen in Figure 3. Many useful devices were made using glass only; recent chips have used silicon capillary breaks made by deep reactive ion etching. Figure 4b shows an example of a silicon capillary break hole; there is no observable breakout. Silicon features also have much more reproducible shape and size.

To make more sensitive measurements of the capillary break response, we used a laser displacement sensor to measure the meniscus height versus applied pressure. Figure 5 shows the result using DMF and the theoretical curve—fit using offsets to the measurements of pressure, P, and height, h, according to the following equation:

$$h = h_0 + \frac{2\gamma}{P + P_0}\left(1 - \sqrt{1 - \left(\frac{r(P + P_0)}{2\gamma}\right)^2}\right), \qquad (2)$$

where r is the radius of the capillary break. The offsets used were h_0 = 4 µm and P_0 = -0.6"; these are consistent with the experimental difficulty in determining the absolute location and pressure at the capillary break.

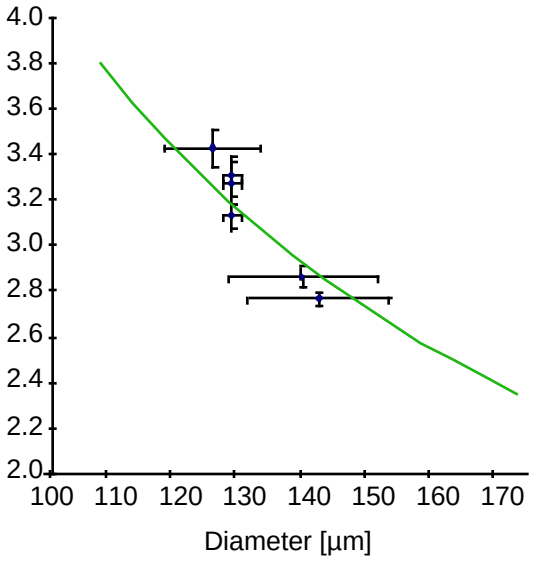

Figure 3: Measured yielding pressure of various capillary breaks. Vertical error bars are the standard deviation of the average yield pressure (5 measurements typical), horizontal error bars are the difference in the measured diameter along the x and y axes. (note: 1" of water = 249 Pa)

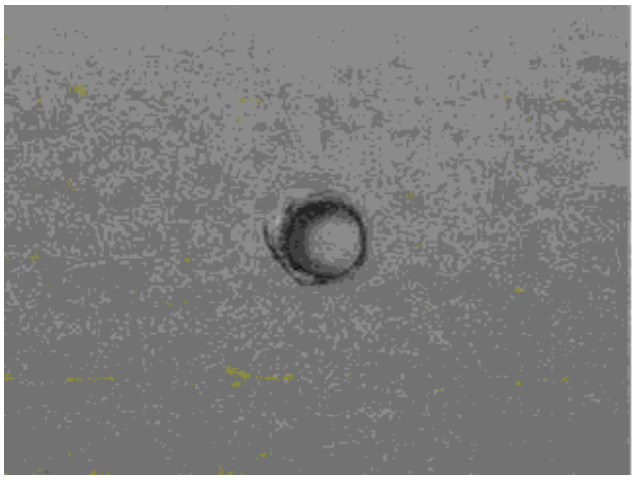

(a)

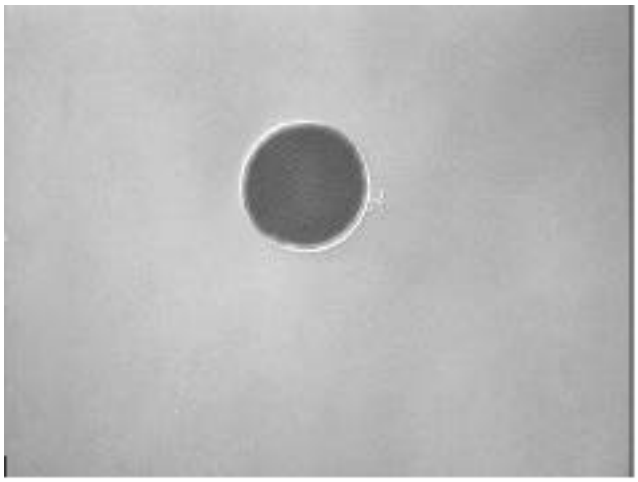

(b)

Figure 4: Capillary break feature: (a) glass, 60 µm diameter, (b) silicon, 75 µm diameter.

CAPACITANCE MODEL

Building off of the simulation and experimental work, we have extended the analytical model of the capillary break operation. As the meniscus area enlarges with increasing pressure, the increase in surface energy appears as a capacitance in the equivalent electrical circuit. The fluidic capacitance relates volume to pressure the same way electrical capacitance relates charge to voltage.

The volume of fluid in the capillary break meniscus, V, is sketched in Figure 6; note that r is the radius of the circular opening, and R is the radius of curvature of the spherical meniscus. The pressure across the meniscus is

$$P = \frac{2\gamma}{R}. \qquad (3)$$

As the volume increases, the curvature, R, decreases until it reaches a minimum value (of r) when the meniscus is half of a sphere. At this point, the pressure is a maximum and we define normalization variables P_{max} and V_{max} as

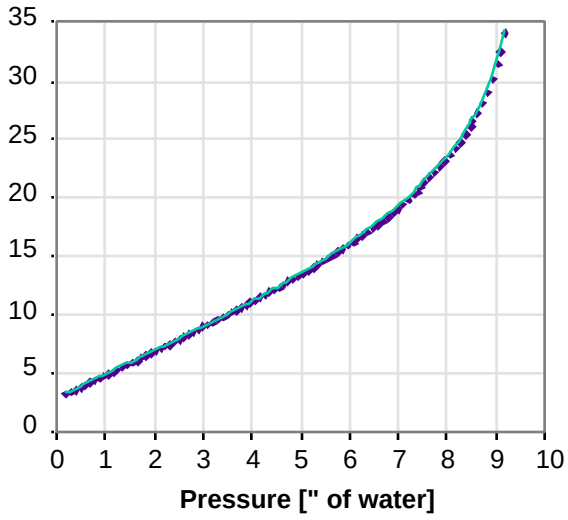

Figure 5: Measured meniscus height versus pressure, including theoretical fit using an adjustable offset in both pressure and height. (note: 1" of water = 249 Pa)

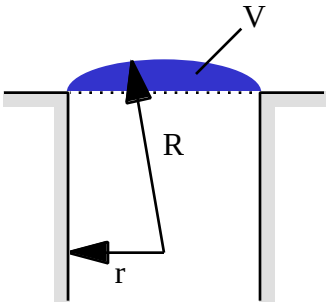

Figure 6: Sketch of the meniscus volume (shaded region).

$$P_{max} = \frac{2\gamma}{r}, \quad V_{max} = \frac{2}{3}\pi r^3. \qquad (4)$$

Writing normalized pressure as P' and normalized volume as V', it can be shown that the meniscus volume as a function of pressure is

$$V' = \left[\frac{1-\cos\left(\sin^{-1}(P')\right)}{(P')^3} - \frac{\cos\left(\sin^{-1}(P')\right)}{2P'}\right] \qquad (5)$$

The volume given by Equation 5 is plotted in Figure 7. Because the increase in meniscus volume with pressure is nonlinear, the capacitance is also nonlinear. However, for a contact angle of less than 30° or for small pressures the capacitance is approximately constant and given by:

$$C = \frac{3}{8}\frac{V_{max}}{P_{max}} = \frac{\pi r^4}{8\gamma}. \quad (6)$$

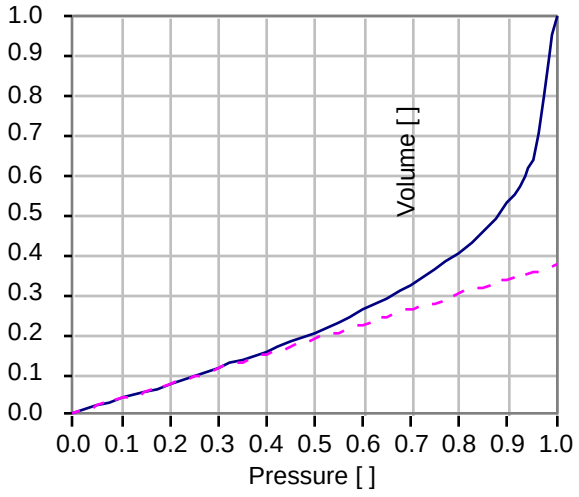

Figure 7: Normalized meniscus volume versus normalized pressure. The dashed line is the linear approximation; the slope represents the meniscus capacitance.

For *P'* less than 0.5, the deviation from the linear approximation is at most 8%.

CONCLUSIONS

The capillary break is well described by simple equations for its static and dynamic behavior that have been verified experimentally. The model has been developed with significant contributions from CFD, analytical calculations, and experiments. Combining the capillary break capacitance model with a fluid channel (represented by a resistance for viscous losses, and an inductance for fluid inertia) gives an equivalent circuit of the fluid channels tested here. Moving forward, we are studying larger, more complicated networks in SPICE simulations to understand design tradeoffs and dynamic system performance.

ACKNOWLEDGMENTS

This work has been supported by SmithKline Beecham Pharmaceuticals and Orchid Biocomputer, Inc.

REFERENCES

[1] P. Gravesen, J. Branebjerg and O. S. Jensen, J. *Micromech. Microeng.*, **3**, 168–182, 1993.

[2] R. L. Columbus and H. J. Palmer, *Clin. Chem.*, **33**/9, 1531–1537, 1987.

[3] Z. H. Fan, R. Kumar, G. Deffley, Q. Dong, P. Stabile, T. Fare, "Oligonucleotide Ligation Reactions on a Chip Using Magnetic Particles," presented at the 1998 Solid-State Sensor and Actuator Workshop (Hilton Head, SC, 8–11 June 1998, pp. 97–100).

[4] R. C. Anderson, G. J. Bogdan, A. Puski, and X. Su, "Genetic Analysis Systems: Improvements and Methods," presented at the 1998 Solid-State Sensor and Actuator Workshop (Hilton Head, SC, 8–11 June 1998, pp. 7–10).

[5] L. Bousse, A. Kopf-Sill, and J. W. Parce, "An Electrophoretic Serial to Parallel Converter," presented at the 1997 International Conference on Solid-State Sensors and Actuators (Chicago, IL, 16–19 June 1997, pp. 499–502).

[6] W. H. Moos, "Introduction: Combinatorial Chemistry Approaches the Next Millennium," in *A Practical Guide to Combinatorial Chemistry*, A. W. Czarnik and S. H. DeWitt, Eds., American Chemical Society, 1997.

[7] S. E. McBride, R. M. Moroney and W. Chiang, "Electrohydrodynamic Pumps for High-density Microfluidic Arrays," presented at Micro Total Analysis Systems '98 (Banff, Canada, 13–16 October 1998, pp. 45–48, Kluwer Academic Publishers).

[8] *FLUENT*, Fluent, Inc. (Lebanon, New Hampshire).